Study of (p,pn) Reactions in Medium Weight Nuclei at 370 MeV*

L. P. REMSBERG†‡ AND J. M. MILLER
Columbia University, New York, New York
(Received 22 January 1963)

Cross sections for the (p,pn) reaction at a proton energy of 370 MeV have been measured with Sc^{45}, Cr^{50}, Cr^{52}, Mn^{55}, Fe^{56}, Ni^{58}, Co^{59}, Cu^{65}, Ga^{69}, and Ga^{71} targets. All of the (p,pn) cross sections, except those for Sc^{45}, Cr^{50}, and Ni^{58}, were found to be about 60 mb. No quantitative explanation could be found for these three divergent cross sections, all of which are lower than the others. Cross sections for $(p,2n)$ reactions on Cr^{52} and Fe^{56} were also measured. Calculations based on the $(p,2n)$–(p,pn) ratio show that at least 85% of the (p,pn) reactions proceed by a pure knock-on mechanism.

I. INTRODUCTION

NUCLEAR reactions initiated by high-energy protons ($E_p>100$ MeV) have been successfully interpreted in terms of a two step model.[1] The first step is a series of binary collisions between the incident proton and individual nucleons in the target nucleus; the struck nucleons can also make further collisions in the target nucleus. This direct interaction step, or cascade, results in the ejection of a number of nucleons which, then, leaves an excited residual nucleus. The second step is the de-excitation of the excited residual nucleus by the emission of particles and gamma rays yielding the final product nucleus. This is usually referred to as the evaporation step. Details of the mechanisms of high-energy spallation reactions are somewhat obscured by the statistical nature of both the cascade and evaporation steps. The situation is further complicated because, in general, any particular product can be formed by a variety of pathways. Details of simple nuclear reactions, in which the product nucleus differs from the target nucleus by no more than one mass number, should be easier to understand since only one target nucleon will be involved in the cascade, and no more than one nucleon will be evaporated.

The (p,pn) reaction has been the subject of more radiochemical investigations than any other simple nuclear reaction.[2–9] These have shown that (p,pn) cross sections are relatively large, about 10% of the total reaction cross section, and exhibit little energy dependence from about 200 MeV to several BeV. Of particular interest is the work of Markowitz *et al.*[3] in which it was reported that (p,pn) cross sections for certain targets within a narrow range of mass numbers appeared to fall in two groups. They found that the cross sections for Fe^{54} and Ni^{58} were about 30% less than the cross sections for Cu^{63}, Zn^{64}, and Cu^{65}.

It has been suggested[2,7,8,10] that the (p,pn) reaction at high energies takes place predominantly by a direct knock-on mechanism, i.e., a (P,PN) cascade with no subsequent evaporation. The alternative mechanism is one in which only one nucleon is emitted in the cascade which is then followed by the evaporation of the other nucleon. The $(p,2n)$ reaction is expected to proceed nearly completely by this second mechanism. A $(P,2N)$ cascade is possible, but since this requires two collisions within the target nucleus, the probability that the residual nucleus is left with insufficient excitation energy to evaporate another particle is small. Thus, the ratio of the (p,pn) to the $(p,2n)$ cross sections for a given target nuclide can be used to estimate the extent to which the (p,pn) reaction goes by the second mechanism.

The purpose of this work was to investigate the variations of (p,pn) cross sections for targets with mass numbers around 60. It was necessary not only to measure several (p,pn) cross sections in this mass region, but to measure them quite accurately in order to characterize the variations and possibly to determine what factors influence these cross sections. The targets chosen were: Sc^{45}, Cr^{50}, Cr^{52}, Mn^{55}, Fe^{56}, Ni^{58}, Co^{59}, Cu^{65}, Ga^{69}, and Ga^{71}. The $(p,2n)$ cross sections were measured for Cr^{52} and Fe^{56} in order to determine the relative importance of the two general mechanisms for the (p,pn) reaction.

II. EXPERIMENTAL PROCEDURES

All targets were irradiated in the internal proton beam of the Nevis Synchrocyclotron at a radius corresponding to a nominal energy of 380 MeV. The radial oscillations of the beam were measured indirectly and were found to produce an energy spread of 16–20 MeV. The energy spread caused by multiple traversals is estimated to be less than 5 MeV and, when combined with that due to radial oscillations, gives an average

* Research supported in part by the U. S. Atomic Energy Commission.
† Present address: Brookhaven National Laboratory, Upton, New York.
‡ Submitted in partial fulfillment of the requirements for the degree of Doctor of Philosophy in the Faculty of Pure Science, Columbia University.
[1] J. M. Miller and J. Hudis, Ann. Rev. Nucl. Sci. **9**, 159 (1959).
[2] A. A. Caretto and G. Friedlander, Phys. Rev. **110**, 1169 (1958).
[3] S. S. Markowitz, F. S. Rowland, and G. Friedlander, Phys. Rev. **112**, 1295 (1958).
[4] H. P. Yule and A. Turkevich, Phys. Rev. **118**, 1591 (1960).
[5] I. M. Ladenbauer and L. Winsberg, Phys. Rev. **119**, 1368 (1960).
[6] P. P. Strohal and A. A. Caretto, Phys. Rev. **121**, 1815 (1961).
[7] S. Singh and J. M. Alexander, Phys. Rev. **128**, 711 (1962).
[8] E. R. Merz and A. A. Caretto, Phys. Rev. **126**, 1173 (1962).
[9] N. T. Porile, Phys. Rev. **125**, 1379 (1962).
[10] E. Belmont and J. M. Miller, Phys. Rev. **95**, 1554 (1954).

TABLE I. Target composition.

Target		Isotopic abundance	Chemical form
Sc^{45}	(natural)	100%	Sc_2O_3 powder
Cr^{50}	(enriched)	88%	Cr_2O_3 powder
Cr^{52}	(enriched)	99.1%	K_2CrO_4 powder
Mn^{55}	(natural)	100%	Mn powder
Fe^{56}	(natural)[a]	91.7%	Fe foil
Fe^{56}	(enriched)[b]	99.7%	Fe_2O_3 powder
Co^{59}	(natural)	100%	Co powder
Ni^{58}	(enriched)	99.6%	NiO powder
Cu^{65}	(natural)	30.9%	Cu foil
Ga^{69}	(enriched)	98.4%	Ga_2O_3 powder
Ga^{71}	(natural)	39.5%	Ga_2O_3 powder

[a] Used for $Fe^{56}(p,pn)Fe^{55}$.
[b] Used for $Fe^{56}(p,2n)Co^{55}$.

proton energy through the targets of about 370 MeV with a maximum spread of plus and minus 10 MeV.

The compositions of the targets are listed in Table I. Two types of targets were used: metal foils and powders. The foil targets consisted of a stack of three 1-mil aluminum foils, the target foils, and three more aluminum foils. These foils were all cut to the same size and aligned as accurately as possible in the target holder. The two foils adjacent to the target foil were discarded, and the activities of the remaining four monitor foils were averaged. The activities of the two outside foils were corrected for recoil loss.[11]

The powder targets were prepared by allowing a slurry of the finely ground target material suspended in absolute ethanol to settle in a rectangular depression (0.3 cm×2.2 cm×0.1 cm deep) in 1-mil aluminum foil. The bottom of the depression, which was made with a machined die and stamping tool, was flat and the sides were straight so that a well-defined target could be prepared. Targets of acceptable uniformity were oven dried, weighed, and when necessary covered with a few drops of 10% Duco cement in acetone. The aluminum monitor foils had depressions which were identical with those used for making targets, and a stock of these foils fit together very snugly which insured precise alignment. The assembled stack was similar to that for the foil targets except that the first and last aluminum foils were part of an aluminum envelope around the other foils and the target. The middle foils of each group of three aluminum foils were used for monitors, and after an irradiation, the bottoms of the depressions of the monitor foils were carefully cut out for disintegration rate determinations. Errors due to imperfect cutting were partly compensated by weighing each monitor foil and putting the monitoring on an activity per unit mass basis. The depressions, which define the target and the monitor foils, were about $\frac{1}{16}$ in. away from the leading edge of the assembled target stack. Thus, the region near the leading edge where the variations in beam intensity are largest is not used. This improvement in the uniformity of the beam through the actual target reduces errors introduced by nonuniform targets and imprecise cutting of the monitor foils.

The production of Na^{22} in the aluminum monitor foils was used to measure the effective beam current through each target. The cross section for the $Al^{27}(p,3p3n)Na^{22}$ reaction was determined relative to that of the $Al^{27}(p,3pn)Na^{24}$ reaction; hence the cross sections in this work were actually measured relative to the $Al^{27}(p,3pn)Na^{24}$ cross section.

Standard chemical separation procedures were used to isolate all the products studied in this work. When the determinations of the disintegration rates of the various products were completed, the samples were dissolved and the chemical yields were determined by spectrophotometric methods.[12]

The methods used for the determination of disintegration rates were chosen to give the greatest possible accuracy consistent with the decay-scheme data that are available. The decay data[13] which are pertinent to these determinations are listed in Table II.

The disintegration rates of the positron emitters were determined with the positron-annihilation-radiation-coincidence-method. The two annihilation quanta were detected with two 2-in.×2-in. NaI scintillation crystals. The efficiency for detecting positrons was determined with a calibrated Na^{22} standard. When coincidences between one annihilation gamma and a nuclear gamma or between two nuclear gammas, as well as summing events in one crystal, are properly accounted for, an accuracy of 2–3% can be attained with this method. It is described in more detail in the Appendix.

TABLE II. Disintegration data of observed nuclides.

Nuclide	$t_{1/2}$	Radiation used for disintegration rate determinations	Fraction of total decay
Na^{22}	2.58 years	(calibrated by beta-gamma coinc. meas.)[a]	
Na^{24}	15.0 h	(calibrated by beta-gamma coinc. meas.)	
Sc^{44g}	3.95 h	positron	0.915
Sc^{44m}	2.46 days	Sc^{44g} daughter	1.00
Cr^{49}	42.0 min	positron	0.92[b]
Cr^{51}	27.8 days	0.323 MeV gamma	0.098
Mn^{51}	45.0 min	positron	0.96
Mn^{52g}	5.6 days	positron	0.29[c]
Mn^{52m}	21.0 min	positron	0.98[b]
Mn^{54}	291 days	0.840 MeV gamma	1.00
Fe^{55}	2.70 years	K x ray (EC)	0.239
Co^{55}	18.0 h	positron	0.79
Co^{56}	77.3 days	0.845 MeV gamma	1.00
Co^{57}	267 days	0.137 and 0.123 MeV gammas	0.98
Co^{58}	71.3 days	(calibrated by beta-gamma coinc. meas.)	
Ni^{57}	36.0 h	positron	0.47
Cu^{64}	12.8 h	positron	0.187
Ga^{65}	15.0 min	positron	0.81
Ga^{66}	9.45 h	positron	0.513
Ga^{68}	68.0 min	positron	0.875
Ga^{70}	21.0 min	negatron	1.00

[a] The fraction of decays which go by positron emission is 0.898.
[b] These values were computed from the theoretical capture to positron ratios given by M. L. Perlman and M. Wolfsberg, BNL 485 (T-110) 1958, (unpublished) and the L/K capture ratios given by reference 18.
[c] This was determined as part of this work.

[11] S-C. Fung and I. Perlman, Phys. Rev. 87, 623 (1952).

[12] E. B. Sandell, *Colorimetric Determination of Traces of Metals* (Interscience Publishers, Inc., New York, 1950), 2nd ed.

[13] *Nuclear Data Sheets*, compiled by K. Way *et al.* (Printing and Publishing Office, National Academy of Sciences–National Research Council, Washington 25, D. C., 1961).

TABLE III. Individual cross sections (mb).

Target	(p,pn)	$(p,2n)$	$(p,2p)$	(p,n)	$(p,p2n)$	$(p,p3n)$
Sc^{45}	34.1					
	35.9					
	33.5					
Cr^{50}	47.8					
	45.6					
	51.1					
Cr^{52}	59.2					
	58.2	0.86		1.43		5.6
	60.3	0.80		1.46		6.2
	58.9					
Mn^{55}	58.7					
	62.1					
	62.6					
Fe^{56}	61.3	0.76		0.90		
	68.0	0.79		0.95		
	62.4	0.76		0.91		
Ni^{58}	30.7		32.8			
	29.4		31.4			
	28.7		32.8			
	28.4					
Co^{59}	55.4				36.6	11.4
	54.6				35.5	11.1
	63.0				41.5	12.9
Cu^{65}	58.0					
	57.7					
	60.0					
Ga^{69}	57.9					
	60.4					
	56.8					
Ga^{71}	59.0					
	54.0					
	61.2					
	58.4					

The disintegration rates of the gamma emitters were determined with a NaI scintillation spectrometer by direct comparison with calibrated standards. Some of these standards were calibrated directly by beta-gamma coincidence measurements, as indicated in Table II; the Co^{57} standard was calibrated with a 4π NaI scintillation detector[14]; and the others were calibrated with a 2-in.×2-in. NaI scintillation crystal. This crystal was calibrated over a wide range of gamma energies with a series of standards whose disintegration rates were determined by beta-gamma coincidence measurements. The accuracy of all of these calibrations was better than 3%.

A brass, side-window, 4-in.-diam x-ray proportional counter,[15] filled with 90% Ar–10% CH_4 at one atmosphere, was used in the determination of the Fe^{55} disintegration rates. An aluminum baffle with a hole 0.5 in. in diameter just below the window served to define the geometry precisely. Corrections for the absorption of the Mn K x rays in the sample, the cellophane cover, air, and the beryllium window were made, and the efficiency of the counter was calculated from the absorption of the x rays in Ar and CH_4.[16] The fluorescence yield of Mn was taken as[17] 0.260 and the L/K capture ratio as[18] 0.09.

The disintegration rates of the Ga^{71} samples were determined with an end-window flow proportional counter using 78% He–22% CH_4 as the counting gas. The maximum energies of the Ga^{68} and Ga^{70} betas are about the same, and the difference between positron and negatron back-scattering has been shown to be less than 3% for the arrangement used in this laboratory.[19] Thus, the detection efficiency of the proportional counter for these two nuclides should be identical. The efficiency of the counter for the Ga^{68} present in each Ga^{70} sample was determined with the positron annihilation coincidence counter; thus, the efficiency of the counter for Ga^{70} was determined for each sample. The accuracy of this procedure was about 5%.

III. RESULTS

All of the cross sections were calculated relative to the cross section for the production of Na^{22} in the aluminum monitor foils; these ratios were then multiplied by the ratio of the cross section for the production of Na^{22} to that of Na^{24} from aluminum to give the cross sections relative to that of the $Al^{27}(p,3pn)Na^{24}$ monitor reaction. The average of a large number of independent measurements of the Na^{22}/Na^{24} cross-section ratio at 370 MeV gave a value of 1.46±0.03. The individual cross sections were based on a value of 11.0 mb for the $Al^{27}(p,3pn)Na^{24}$ reaction and are listed in Table III.

The averages of the individual determinations of the various (p,pn) cross sections are listed in Table IV. The standard deviations of the individual cross sections that are also given were calculated from the spread of values obtained from the three or four measurements of each cross section. The uncertainty in an individual

TABLE IV. (p,pn) cross sections and standard deviations, in mb.

Target	Average cross section and combined standard deviation	Standard deviation of the individual cross sections (%)	Standard deviation of systematic errors (%)
Sc^{45}	34.5±1.6[a]	3.6	4.2
Cr^{50}	48.2±2.9	5.7	5.0
Cr^{52}	59.2±4.5	1.5	7.6[b]
Mn^{55}	61.1±2.3	3.5	3.1
Fe^{56}	63.9±3.8	5.6	5.0
Ni^{58}	29.4±1.0	3.5	3.1
Co^{59}	57.7±3.2	8.0	3.0
Cu^{65}	58.6±3.3	2.1	5.5[c]
Ga^{69}	58.4±2.6	3.2	4.0
Ga^{71}	58.2±4.3	5.2	6.8

[a] The ratio, Sc^{44m}/Sc^{44g}, was 0.48 for this reaction.
[b] Includes 7% from the branching ratio for the 0.323-MeV gamma.
[c] Includes 5% from the positron branching ratio.

[14] A. E. Metzger and J. M. Miller, Phys. Rev. **113**, 1125 (1959).
[15] W. Bernstein, H. G. Brewer, and W. Rubinson, Nucleonics **6**, No. 2, 39 (1950).
[16] A. H. Compton and S. K. Allison *X-rays in Theory and Experiment* (D. Van Nostrand, Inc., New York, 1935). *Handbook of Chemistry and Physics* (Chemical Rubber Publishing Company, Cleveland, 1951), 33rd ed.
[17] A. H. Wapstra, G. S. Nijgh, and R. Van Lieshout, *Nuclear Spectroscopy Tables* (Interscience Publishers, Inc., New York, 1959).
[18] H. Brysk and M. E. Rose, Rev. Mod. Phys. **30**, 1169 (1958).
[19] K. Rind (private communication).

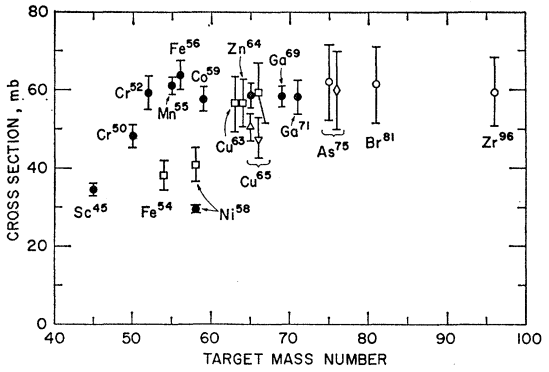

FIG. 1. Cross sections for (p,pn) reactions at 350–400 MeV vs target mass number. ●, this work; □, reference 3 (these cross sections have been reduced by a factor of 0.80 from the published values; (private communication from S. S. Markowitz); ○, reference 6; △, reference 4; ▽, reference 8; ◇, J. B. Cumming, NYO 6141 (1954) and (private communication). The latter two points and the Cu^{65} point from reference 3 have been displaced one mass number. All of these cross sections have been adjusted for a $Al^{27}(p,3pn)Na^{24}$ monitor cross section of 11.0 mb.

cross-section results from the precision of disintegration-rate determinations, precision of chemical yields, decay-curve resolutions, target nonuniformity and misalignment, and, perhaps, other sources which are difficult to identify. In these measurements the disintegration-rate precision was always better than 1%, and the precision of the chemical yields was about 1%. Complex decay-curves were resolved by a least squares program written for the IBM 650 computer; these decay-curve analyses introduced significant uncertainties only in the case of Ga^{71}. It is entirely reasonable to ascribe the remaining uncertainty (about 4% on the average) to target nonuniformity and misalignment.

There are a number of possible systematic errors which will affect the accuracy of the average cross sections. These include uncertainties in the calibrations of the detectors used for absolute disintegration-rate determinations, uncertainties in the calibrations of the chemical-yield procedures, and uncertainties in the decay schemes of the product nuclides. These were estimated as accurately as possible and the root mean square combinations are listed in Table IV. The error in the cross section for the monitor reaction was not included since these (p,pn) cross sections are primarily of interest when they are compared with each other.

The standard deviations calculated for the individual cross sections were divided by the square root of the number of determinations to give the standard deviations of the average cross sections and then combined with the estimated systematic errors to yield the standard deviations listed with the average cross sections in Table IV. The same treatment was applied to the other cross sections listed in Table III, and the averages of these cross sections and their standard deviations are presented in Table V.

IV. DISCUSSION

Two general conclusions can be drawn from the (p,pn) cross sections given in Table IV: (i) Large abrupt variations in (p,pn) cross sections occur for targets within a narrow range of mass numbers: The cross sections for Sc^{45}, Cr^{50}, and Ni^{58} are considerably lower than any of the others. (ii) The other seven cross sections are essentially identical. The average of these seven cross sections is 60 mb, and each differs from this average by less than its own standard deviation.

The (p,pn) cross sections are plotted against target mass number in Fig. 1 along with some other measurements at similar proton energies. The other data do not alter the conclusions stated above; with the other data included, there are 12 (p,pn) cross sections which are very nearly 60 mb and 4 which are lower. The cross section for Cu^{65} of Markowitz *et al.*[3] is in good agreement with that of this work; the cross sections for this target reported by Yule and Turkevich[4] and Merz and Caretto[8] are in fair agreement. There is a large discrepancy between the cross section for Ni^{58} of this work and that of Markowitz *et al.*[3]

Mechanisms of (p,pn) Reactions

There are three plausible mechanisms for (p,pn) reactions at this energy, and each is expected to contribute to the observed cross section.

(A) The incident proton initiates a (P,PN) cascade[20] leaving the residual nucleus with insufficient energy to evaporate any particles (less than about 10 MeV). This would be a "clean knockout" of a target neutron by the incident proton.

(B) A (P,P') cascade leaving the residual nucleus with enough excitation energy for the evaporation of only one nucleon is followed by the emission of one neutron. This will be referred to as $(P,P'n)$.

TABLE V. Additional cross sections, in mb.

Reaction	Average cross section and standard deviation
$Cr^{52}(p,n)Mn^{52}$	1.45±0.10[a]
$Cr^{52}(p,2n)Mn^{51}$	0.83±0.07
$Cr^{52}(p,p3n)Cr^{49}$	5.9 ±0.6
$Fe^{56}(p,n)Co^{56}$	0.92±0.06
$Fe^{56}(p,2n)Co^{55}$	0.77±0.08[b]
$Ni^{58}(p,2p)Co^{57}$	32.3 ±1.3
$Co^{59}(p,p2n)Co^{57}$	37.9 ±3.2
$Co^{59}(p,p3n)Co^{56}$	11.8 ±1.0
$Ga^{69}(p,p3n)Ga^{66}$	18.2 ±1.1
$Ga^{69}(p,p4n)Ga^{65}$	4.5 ±1.5
$Ga^{71}(p,p3n)Ga^{68}$	37.8 ±2.4
$Ga^{71}(p,p5n)Ga^{66}$	10.0 ±0.7

[a] The ratio, Mn^{52m}/Mn^{52g}, was 0.91 for this reaction.
[b] This includes a 10% uncertainty from the positron branching ratio.

[20] Over-all reactions are given in lower case letters; e.g., (p,pn), and cascades are given in capital letters; e.g., (P,N). A mixture of capitals and lower case letters is used to distinguish between cascade nucleons and evaporated nucleons; e.g., (P,Np).

(C) A (P,N) cascade is followed by the evaporation of one proton. This will be referred to as (P,Np).

A (P,PN) cascade occurs when the incident proton collides with a neutron in the target nucleus, and both particles leave the nucleus. The (P,P') and (P,N) cascades occur when the incident proton collides with a nucleon in the nucleus in such a way that one of the collision partners escapes from the nucleus with most of the incident energy; the other collision partner remains in the nucleus. The probability that any of the outgoing nucleons in these cascades undergoes an additional collision without either expanding the cascade or leaving too much excitation energy in the residual nucleus is small. This suggests that (p,pn) reactions occur near the surface of the nucleus.

Inelastic proton-nucleon collisions involving pion production occur at this energy and can produce cascades equivalent to those in the three mechanisms responsible for (p,pn) reactions. The fraction of collisions which are inelastic is small; at 400 MeV about 10% of the proton-proton collisions and 5% of the proton-neutron collisions are inelastic. Inelastic collisions have less chance of producing one of the above cascades than do elastic collisions because there is one more particle to escape from the nucleus without colliding with any nucleons. Furthermore, the total energy available to the particles after the collision is reduced by the rest mass of the pion (140 MeV) and is divided three ways. The mean free paths of nucleons in nuclear matter decrease with decreasing energy, so the probability that the nucleons leave the nucleus without additional collisions is smaller for inelastic events. Thus, it is felt that inelastic processes make no appreciable contribution to (p,pn) reactions at this energy.

It has long been thought that (p,pn) reactions proceed primarily by a direct knock-on mechanism [mechanism (A)] at this energy.[2,7,8,10] The fraction that does go by this mechanism has never been determinated; indeed, it has never been conclusively demonstrated that this mechanism does predominate over the others. The $(p,2n)$ reaction appears to provide a means of determining the relative contributions of the three mechanisms to the (p,pn) reaction.

In contrast to the (p,pn) reaction, the $(p,2n)$ reaction has essentially only one mechanism: a (P,N) cascade followed by the evaporation of one neutron. As mentioned before, the probability of obtaining a $(P,2N)$ cascade product with insufficient excitation for the evaporation of another particle is very small. The ratio of the cross section for process C to that of the $(p,2n)$ reaction, $\sigma(P,Np)/\sigma(P,Nn)$, is the ratio of the probability for the emission of one and only one proton to that for the emission of one and only one neutron from the excited nuclei following (P,N) cascades. This can be calculated with the aid of nuclear evaporation theory.

The ratio of (P,P') cascades followed by the evaporation of one nucleon to (P,N) cascades followed by the evaporation of one nucleon, $\sigma(P,P'x)/\sigma(P,Nx)$, can be calculated from the nucleon-nucleon differential scattering cross section. Since $\sigma(P,Nx)$ is the sum of the $(p,2n)$ cross section and the (P,Np) cross section, $\sigma(P,P'x)$ can then be obtained. The cross section for mechanism B, $\sigma(P,P'n)$, is simply $\sigma(P,P'x)$ multiplied by the probability for the evaporation of one and only one neutron from the excited nuclei following (P,P') cascades. This can also be calculated from evaporation theory. Thus, by measuring both (p,pn) and $(p,2n)$ cross sections for a given target, one can calculate the relative contributions of mechanisms (A), (B), and (C) to the (p,pn) reaction. To the extent that the direct process, $(P,2N)$, contributes to the total $(p,2n)$ cross section, the calculation will give upper limits to processes (B) and (C).

The ratio of the relative probabilities of (P,P') and (P,N) cascades followed by the evaporation of one nucleon was calculated as follows. There are two kinds of collisions which can lead to (P,X) cascades in which the residual nuclei have sufficient excitation energy to evaporate one and only one nucleon. In the first, the incident proton undergoes a small-angle scattering off a nucleon in the nucleus and leaves with most of the incident energy. Sufficient energy is transferred to the struck nucleon to provide excitation for the evaporation of one nucleon. In the second, the incident proton undergoes a large-angle scattering and gives most of its energy to the struck nucleon which then leaves the nucleus; the incident proton is, then, captured and the net excitation energy is sufficient for the evaporation of one nucleon. The kinematics of a nucleon-nucleon collision with a center-of-mass scattering angle, θ, are identical to those with a scattering angle, $\pi-\theta$, with the identity of the two outgoing particles exchanged. If the struck particle is a proton, both small angle and large angle scattering (which are indistinguishable in this case) result in a (P,P') cascade. If the struck particle is a neutron, small angle scattering leads to a (P,P') cascade, and large angle scattering leads to a (P,N) cascade.

The energy transferred in a nucleon-nucleon collision within a nucleus depends not only on the c.m. scattering angle but also on the energy of the struck nucleon, the angle its motion makes with that of the incident proton, and the azimuthal scattering angle. Thus, for a given center of mass scattering angle, there will be a distribution of energy transfers. Since the distributions of neutron and proton momenta within the nucleus are similar, the distributions of energy transfers and hence the distributions of excitation energies will be similar for both (P,P') and (P,N) cascades. The probability that the outgoing nucleon makes no further collisions will be the same for both protons and neutrons only for nuclei with N equal to Z. This is very nearly the case

for both Cr^{52} and Fe^{56}. The distribution of center-of-mass scattering angles in nucleon-nucleon collisions is $\sin\theta$ times the appropriate differential scattering cross section. Thus, the ratio, $\sigma(P,P'x)/\sigma(P,Nx)$, is given by

$$\frac{\sigma(P,P'x)}{\sigma(P,Nx)}=\left[Z\int_0^{\pi/2}W(\theta)(d\sigma/d\Omega)_{pp}\sin\theta d\theta+N\int_0^{\pi/2}W(\theta)(d\sigma/d\Omega)_{np}\sin\theta d\theta\right]\Big/N\int_{\pi/2}^{\pi}W(\theta)(d\sigma/d\Omega)_{np}\sin\theta d\theta, \quad (1)$$

where Z and N are the numbers of protons and neutrons in the target nucleus, θ is the center of mass scattering angle, $(d\sigma/d\Omega)$ is the appropriate differential scattering cross section, and $W(\theta)$ is the probability that a collision with a scattering angle, θ, results in an energy transfer appropriate to the evaporation of one nucleon. The differential scattering cross sections were taken from the compilation by Hess.[21] There is no factor of 2 in the proton-proton term in Eq. (1) since $(d\sigma/d\Omega)_{pp}$ is an experimental quantity and already contains this factor.

$W(\theta)$ is very laborious to calculate directly. An estimate of it was obtained by calculating a large number of energy transfers with relativistic collision mechanics for a variety of c.m. scattering angles. At each scattering angle all the other parameters were varied systematically to get an approximation of the distribution of excitation energies at that scattering angle. The Pauli principle, which requires that the energy transfer be greater than the difference between the binding energy of the struck nucleon and the least bound nucleon of the kind which remains in the nucleus after the collision, was taken into account. It is quite clear from these calculations that $W(\theta)$ is very small for θ not between 10° and 40° (not between 140° and 170° for large-angle scattering). Because of the similarity of the shapes of the differential scattering cross sections in this region, the ratio, $\sigma(P,P'x)/\sigma(P,Nx)$, is not very sensitive to $W(\theta)$. For this reason, $W(\theta)$ was assumed to be constant for θ between 10° and 40° and zero for all other θ. [Note that $W(\pi-\theta]=W(\theta)$.] This yields 1.5 ± 0.3 for the ratio, $\sigma(P,P'x)/\sigma(P,Nx)$, for both Cr^{52} and Fe^{56}, the two targets for which $(p,2n)$ cross sections were measured.

TABLE VI. Summary of the calculations of the cross sections for the various mechanisms for the (p,pn) reaction.

	Cr^{52}	Fe^{56}
G_p/G_n[a]	2.2	1.9
G_n'[b]	0.84	0.79
$\sigma(p,2n)$	0.86 mb	0.77 mb
$\sigma(P,Np)$	1.9 mb	1.5 mb
$\sigma(P,P'n)$	3.5 mb	2.7 mb
$\sigma(p,pn)$	59.2 mb	63.9 mb
$\sigma(P,PN)$	53.8 mb	59.7 mb
$\sigma(P,PN)/\sigma(p,pn)$	0.91	0.93

[a] G_p/G_n is the ratio of the probability of the evaporation of one and only one proton to that of one and only one neutron from the residual nuclei following (P,N) cascades.
[b] G_n' is the probability of the evaporation of one and only one neutron from the residual nuclei following (P,P') cascades.

[21] W. N. Hess, Rev. Mod. Phys. **30**, 368 (1958).

The evaporation calculations were carried out with the expressions and parameters used by Dostrovsky, Fraenkel, and Friedlander.[22] The quantities calculated were the ratio of the probability of the evaporation of one and only one proton to that of one and only one neutron, G_p/G_n, for Mn^{52} and Co^{56}, and the probability of the evaporation of one and only one neutron, G_n', from Cr^{52} and Fe^{56}. The distribution of excitation energies of the residual nuclei following the (P,P') and (P,N) cascades was assumed to be constant. This assumption appears reasonable on the basis of the calculations described in the preceding paragraph. The evaporation calculations were carried out in a manner such that the sensitivity of the calculated quantities to this assumption could readily be observed. It turned out that in this instance none of the four quantities was particularly sensitive to the distribution of excitation energies.

The results of the evaporation calculations are shown in Table VI along with the experimental $(p,2n)$ and (p,pn) cross sections, the calculated $(P,P'n)$ and (P,Np) cross sections, and the ratio $\sigma(P,PN)/\sigma(p,pn)$. This last quantity is the fraction of the (p,pn) reactions that proceed by the direct knock-on mechanism. The (P,PN) cross section [the cross section for mechanism (A)] was obtained by subtracting the $(P,P'n)$ and (P,Np) cross sections from the experimental (p,pn) cross section. Since the calculated $(P,P'n)$ and (P,Np) cross sections are quite small with respect to the measured (p,pn) cross section, large uncertainties in the calculations will have a relatively small effect on the result that at least 90% of the (p,pn) reaction occurs by the direct knock-on mechanism.

Low-energy secondary protons may make significant contributions to the measured $(p,2n)$ cross sections. From the Monte Carlo calculations of Metropolis *et al.*[23] on secondary proton production, an upper limit of 20% may be placed on the contribution of secondaries to the measured $(p,2n)$ cross sections. An error that is this large would hamper a study of $(p,2n)$ reactions, but it has a negligible effect on the previous calculations based on the $(p,2n)$ cross sections.

This analysis neglects processes other than proton-nucleon collisions which can result in (p,p') inelastic scattering. It may be possible that Coulomb excitation by 370-MeV protons may transfer sufficient energy to the nucleus for the evaporation of one nucleon. This

[22] I. Dostrovsky, Z. Fraenkel, and G. Friedlander, Phys. Rev. **116**, 683 (1960).
[23] N. Metropolis, R. Bivins, M. Storm, A. Turkevich, J. M. Miller, and G. Friedlander, Phys. Rev. **110**, 185 (1958).

would make the $(P,P'n)$ cross section larger than that calculated from the $(p,2n)$ cross section, and thus reduce the calculated fraction of (p,pn) reactions that proceed by the direct knock-on mechanism. There is a set of experiments which gives an indication of the extent of Coulomb excitation at a proton energy of 185 MeV.[24] Both the energy and angular distributions of inelastically scattered protons were measured for several targets with Z less than 31. Of particular interest was a broad peak at an excitation energy of about 15–20 MeV, observed for all targets, which showed a proton angular distribution which was sharply peaked forward. This peak, which is apparently identified with the giant resonance in photonuclear reactions, was attributed at least in part to Coulomb excitation. Integration of this peak over both energy and solid angle gave a cross section of about 2 mb for all targets from phosphorus to zinc. Since the excitation is in the range of 15–20 MeV, one nucleon will be evaporated, and this mechanism will contribute to the (p,pn) cross section. If the cross section at 370 MeV is not more than 2–3 times the value at 185 MeV, it still can be concluded that at least 85% of the (p,pn) reactions proceed by the direct knock-on mechanism.

Note added in proof. The differential cross sections for producing the giant resonance peaks observed by Tyren and Maris have been reasonably well reproduced by a theoretical calculation of high-energy Coulomb excitation [M. Kawai and T. Terasawa, Prog. Theoret. Phys. (Kyoto) **22**, 513 (1959)]. This calculation predicts the total cross section for this process to be inversely proportional to the energy of the incident proton.

Variations in (p,pn) Cross Sections

There are several remarks which can be made concerning the variations in the (p,pn) cross sections in this mass region: (1) There is apparently a "normal" (p,pn) cross section of 60 mb. (2) Those observed cross sections which differ from this value are all smaller and occur for targets with a mass number less than 59. (3) The cross sections do not vary smoothly with either the mass number or the neutron number of the target. (4) With the exception of Sc^{45}, all of the targets with low (p,pn) cross sections are well out on the neutron deficient side of stability.

In terms of the direct knock-on mechanism, the (p,pn) cross section can be divided into two parts: the probability that the incident proton initiates a (P,PN) cascade, and the probability that the (P,PN) cascade product has insufficient excitation energy to evaporate a nucleon. There is nothing obvious in any reasonable nuclear model which would reduce the probability of obtaining a (P,PN) cascade by as much as the factor of two which is necessary to explain the low cross sections for Sc^{45} and Ni^{58}. These abrupt changes in the observed cross sections must, then, reflect abrupt changes in the excitation-energy spectrum subsequent to a (P,PN) cascade.

To a first approximation, the excitation energy of the residual nucleus following a (P,PN) cascade is equal to the depth of the neutron hole; i.e., the difference between the energy of the neutron which was removed and the energy of the least bound neutron. The number of neutrons in levels sufficiently high so that the removal of one of them does not yield enough excitation for the evaporation of a particle can be determined with the aid of the nuclear shell model and knowledge of the separation energies of the least bound nucleons in the (p,pn) product nuclides. These numbers of "available" neutrons do not, however, correlate with the observed variations in the (p,pn) cross sections. For example, Mn^{55}, Fe^{56}, and Ni^{58} each have 30 neutrons, and they also have similar neutron level-structures according to the shell model. The separation energies of the least bound nucleons in the Mn^{54}, Fe^{55}, and Ni^{57} products are such that the same number of available neutrons is predicted for each target. The (p,pn) cross section for Ni^{58}, however, is about one half that of the other two targets. (The competition between de-excitation by particle emission with de-excitation by gamma-ray emission[25] was considered, but this also could not explain the low cross section for Ni^{58}.)

A quantity which is important for the determination of the distribution among quantum states of the A-1 nucleons that remain after a (p,pn) reaction is the overlap integral between initial and final states for the residual A-1 nucleons. Lane and Wilkinson[26] have pointed out that the overlap integral may, in turn, be expressed in terms of the fractional parentage of the states involved. Thus, in these terms, the three low (p,pn) cross sections reported here imply that states that are stable to particle emission in Sc^{44}, Ni^{57}, and Cr^{49} are less important parents of the ground states of Sc^{45}, Ni^{58}, and Cr^{50}, respectively, than are the corresponding states for the other target nuclides that were studied.

V. CONCLUSIONS

Calculations based on the measured $(p,2n)$-(p,pn) cross section ratio show that at least 85% of the (p,pn) reaction is accounted for by the direct knock-on mechanism, provided that the contribution from Coulomb excitation is small. Abrupt variations in (p,pn) cross sections have been observed for targets in a narrow mass region around mass number 60 and cannot be satisfactorily explained in terms of any known nuclear model.

ACKNOWLEDGMENTS

The authors are indebted to Dr. K. Rind for generous aid in all phases of this work. We wish to thank Dr.

[24] H. Tyren and Th. A. J. Maris, Nucl. Phys. **6**, 446 (1958); **7**, 24 (1958).

[25] J. R. Grover, Phys. Rev. **123**, 267 (1961).

[26] A. M. Lane and D. H. Wilkinson, Phys. Rev. **97**, 1199 (1955).

W. F. Goodell and the staff of the Nevis Cyclotron Laboratory for their cooperation. We also wish to thank Dr. J. R. Grover for some helpful discussions. The financial aid of the National Science Foundation in the form of Predoctoral Fellowships (1956–57 and 1958–59) is gratefully acknowledged by one of us (L.P.R.).

APPENDIX: THE POSITRON ANNIHILATION COINCIDENCE METHOD

The source was tightly sandwiched between sufficient absorbers to stop all of the positrons and placed in a source holder midway between two 2-in.×2-in. NaI scintillation crystals. The outputs of the photomultipliers were connected through conventional electronics to a fast-slow coincidence circuit with single-channel analyzers in each slow channel. The channels were set to accept the 511-keV photopeak from annihilation radiation. The upper level requirements of the single-channel analyzers could be removed so that either the differential or the integral mode could be used.

The efficiency for detecting positrons was determined with a Na^{22} standard sandwiched between the same amount of absorber as the samples. The efficiency for detecting positron annihilation coincidences is a sensitive function of the source diameter, much more so than it is for detecting a single gamma in one NaI crystal. Furthermore, this effect does not decrease as the distance between the source and the detectors is increased, as it does for a single detector. For this reason, the Na^{22} standard was made with the same diameter as the samples.

The contribution to the coincidence counting rate of coincidences between a nuclear gamma and one annihilation gamma and between two nuclear gammas was evaluated by moving one of the detectors around to 90° with respect to the source and the other detector. The probability of getting a coincidence between a nuclear gamma and one annihilation gamma is smaller at 180° than it is at 90° by a factor of one minus the intrinsic photopeak efficiency of the detector for a 511-keV gamma. Thus, any part of the 90° coincidence counting rate which was due to this kind of event was multiplied by this factor (0.7 for 2-in.×2-in. crystals) before it was subtracted from the 180° rate.

It was also necessary to correct for summing events taking place in one crystal. If a nuclear gamma is detected simultaneously with an annihilation gamma photopeak event, the resulting sum pulse will not fall within the 511-keV channel. This effect can be particularly bad if low-energy gammas, which are detected with high efficiency, are present. Published efficiency curves[27] were used to correct for this effect. The fraction of annihilation-annihilation coincidences which are lost due to summing with a nuclear gamma in either crystal is twice the *total* efficiency for detecting the gamma in one crystal. Compton-Compton summing-in events are sufficiently rare to be ignored, but summing between the photopeak of a low-energy gamma and the Compton spectrum of the annihilation radiation to produce counts in the 511-keV channel can be significant.

Most of the summing effects vanish when the circuit is operated in the integral mode. However, gamma-gamma and annihilation-gamma coincidences are minimized in the differential mode. Thus, the choice of the mode of operation is dictated by the decay scheme of the nuclide under consideration. Whenever possible, data was taken in both modes, and, after appropriate corrections, the results usually were within about $1\frac{1}{2}\%$ of each other.

The probability of detecting gamma-gamma and annihilation-gamma coincidences and summing events is inversely proportional to the square of the geometry. (Geometry is the solid angle from the source subtended by one of the detectors.) The probability of detecting an annihilation-annihilation coincidence is inversely proportional to the first power of the geometry. Thus, the percent correction to the 180° counting rate is inversely proportional to the geometry. The largest geometry used in this work was 5% of 4π; in general, the smallest geometry consistent with acceptable counting rates was used.

[27] R. L. Heath, AEC Research and Development Report IDO-16408 (1957).